IEEE Access
Multidisciplinary | Rapid Review | Open Access Journal

Received October 26, 2020, accepted November 30, 2020, date of publication December 9, 2020,
date of current version December 21, 2020.

Digital Object Identifier 10.1109/ACCESS.2020.3043470

Steady-State Model of Pressure-Flow Characteristics Modulated by Occluders in Cardiopulmonary Bypass Systems

HIDENOBU TAKAHASHI[1], ZU SOH[2], (Member, IEEE), AND TOSHIO TSUJI[2], (Member, IEEE)

[1]Department of Medical Science and Technology, Faculty of Health Science, Hiroshima International University, Hiroshima 7392695, Japan
[2]Graduate School of Advanced Science and Engineering, Hiroshima University, Higashihiroshima 7398511, Japan

Corresponding authors: Hidenobu Takahashi (h-taka@hirokoku-u.ac.jp) and Toshio Tsuji (tsuji@bsys.hiroshima-u.ac.jp)

This work was supported by JSPS KAKENHI under Grant 19K12851.

ABSTRACT Cardiopulmonary bypass is a complex procedure that involves the maintenance of heart and lung functions using an external system during cardiac surgery. It is prone to significant human errors, which are mainly caused by inappropriate occluder operation that controls the perfusion balance by adjusting flow rates. Hence, there is a requirement for automatic occluder control; however, the relationship between occluder operation and flow rates remains unclear. The aim of this study is to use a steady-state model to evaluate the influence of occluder control on the flow and pressure of a cardiopulmonary bypass system. Perfusion experiments were performed using Newtonian (glycerin solution) and non-Newtonian (erythrocyte turbid solution) fluids to investigate the pressure-flow characteristics modulated by the occluder. We also visualized the fluid to verify the validity of the measurement data. Based on these experimental data, an exponential occlusion-pressure model is derived to express the relationships between the opening ratio of the occluder and flow rate. Estimation is then achieved by combining the occlusion-pressure model with the linear pressure-flow model. Results reveal that the combined model fitted the perfusion experiment data well for the venous and arterial line side ($R^2 = 0.946$ and 0.985, respectively; $p < 0.01$). Further, leave-one-out cross-validation and Bland–Altman analysis confirmed that the combined model could predict flow rates accurately with minimal proportional and bias errors. Therefore, the proposed model can serve as a basis for the further development of cardiopulmonary manipulation systems.

INDEX TERMS Automatic occluder control, cardiopulmonary bypass systems, experiments, pressure-flow characteristics.

I. INTRODUCTION

Cardiopulmonary bypass (CPB) is a procedure that involves the temporary replacement of heart and lung functions for the maintenance of systemic circulation during cardiac surgery. CPB drains blood from the right atrium and bypasses the circulation of the heart and lungs. This bypass perfuses blood into the systemic circulation from the aorta after the gas exchange in the oxygenator. In the perfusion process, sufficient preservation of systemic blood pressure is critical for organ impairment prevention, especially with respect to their functions [1]. Therefore, a CPB operator is required to carry out delicate operations for the prevention of significant variations in perfusion pressure and to ensure that the arterial- and venous-line side flow rates are equal.

To prevent a decrease in blood pressure owing to abrupt blood removal at the start of CPB [2], in addition to air embolisms owing to low blood retention levels [3], it is necessary to minimize human error and meticulously carry out the CPB procedure. During the first CPB procedure by Gibbon [4], a safety sensor was installed in the reservoir to monitor the perfusion balance between the arterial- and venous-line sides for human operation support, as is currently common practice. Nonetheless, human error is the main cause of CPB accidents, not equipment failure [5], [6]. Thus, complex CPB operations require simplification, automation, or both for the prevention of human error [7], [8].

The associate editor coordinating the review of this manuscript and approving it for publication was Jenny Mahoney.

Therefore, a system that can monitor and automatically control the blood reservoir level by measuring the blood reservoir static pressure was developed [9]. However, it was not practically implemented owing to its requirement of a specialized device and the development of improved disposable blood reservoirs. Moreover, a scheme that can control perfusion on the arterial- and venous-line sides by measuring blood flow on the venous-line side was developed and implemented in clinical applications [10]. However, this scheme can only be applied to CPB systems that employ roller pumps as the supply pump and not centrifugal pumps. Given that the roller pump may lead to abnormal increases in pressure, thus leading to the transfer of a large amount of air [11] to the arterial-line side, gas microemboli are present [12]–[16]. Nevertheless, many hospitals typically use roller pumps as blood pumps, owing to operation complexities when the centrifugal pump is used [17], [18]. In the centrifugal pump, the perfusion balance is adjusted by operating the occluders attached to the venous and arterial lines. The blood flow rate should be estimated from the occluder closure to achieve automatic maintenance of the blood reservoir level.

As reported, the relationship between the differential pressure and Reynolds number can be applied to viscous fluids in general differential pressure flow meters, from which the flow rate from the fluid differential pressure can be obtained using an orifice plate based on Bernoulli's theorem [19]–[21]. Based on these reports, a system that can continuously monitor blood viscosity by measuring the differential pressure and flow rate of the oxygenator was proposed [22]–[24]. Additionally, a mathematical model that can express the relationship between the blood flow rate and differential pressure for perfused viscous fluids was also proposed [25]–[27]. However, the effects of the occluder on the flow rate have not been revealed. If flow rate can be estimated from the operation amount of the occluder, it can serve as a basis for the development of a system that links the venous and arterial line occluder operations, thus simplifying the CPB operation and decreasing the probability of human error [25]. The ultimate goal of this study is to construct an assisted cardiopulmonary manipulation control system that can reduce the burden on the operator. Thus, in this study, we model the relationship between the occluder operation amount and flow rate, which can provide a basis for the control system. Such a model needs to include an occluder operation amount term explicitly and be simple enough for real-time control. Therefore, the model only focused on steady-state flow.

We propose an exponential model to address the relationships between the opening ratio of the occluder and the differential pressure. Combining this model with the previous model [22]–[24], [26], which links differential pressure and flow rate, allows the estimation of the flow rate from the opening ratio of the occluder. The following experiments were carried out to determine the model parameters. First, the occluders on the arterial- and venous- line sides were modulated to investigate the differential pressure-flow rate characteristics of Newtonian (glycerin solution) and non-Newtonian fluids (erythrocyte turbid solution), which were perfused using a CPB system. Additionally, the influence of the fluid viscosity on frictional losses was experimentally investigated with respect to occluder perfusion and viscosity. Finally, we investigated the characteristics of the flow in the blood circuit by visualizing perfusion near the occluder to confirm the validity of the measurement data.

II. MATERIALS AND METHODS

This section describes the *in vitro* experiments using the CPB system, which is shown in Fig. 1.

A. CPB SYSTEM SPECIFICATIONS

The CPB system consisted of an oxygenator (HPO-23H-CP; Senko Medical Instrument Mfg. Co., Ltd., Tokyo, Japan), venous reservoir (HVR-4NFP; Senko Medical Instrument Mfg. Co., Ltd.), and centrifugal pump (CX-SL45X; Terumo Cardiovascular Systems Corp, Tokyo, Japan), which were connected by polyvinyl chloride tubes, thus forming a closed circuit, as shown in Fig. 1. Occluders (HAS-RH200; Senko Medical Instrument Mfg. Co., Ltd., Tokyo, Japan) were attached to the arterial- and venous-line sides of the oxygenator circuit for flow rate regulation. Figs. 2 and 3 show the relationship between the manipulator (HAS-RH200 knob) value and the opening ratio of the occluder d_c/d, where d_c is the length of the tube in the compression direction, and d is the diameter of the original tube. (Data published by Senko Medical Instrument Mfg. Co., Ltd., (Tokyo, Japan)). There are two types of tubes commonly used in cardiopulmonary blood circuits: 10 mm and 12 mm. In both cases, they are reported to behave in such a way that the same curve is drawn. A three-way stopcock was connected to the occluder inlet and outlet, and the pressure was measured from the stopcock using pressure sensors (40PC015, Pressure range 0-15psi, Total accuracy $\pm 0.4\%$; Honeywell Japan, Inc. Tokyo, Japan). Moreover, an electromagnetic blood flow meter (FD-M5AT, Flow range 0-10 L/min, Repetition accuracy 10s: $\pm 1\%$; Keyence Corp, Tokyo, Japan) was installed at the oxygenator outlet.

B. EXPERIMENTAL FLUIDS

A glycerin solution and a human erythrocyte turbid solution were employed as working fluids. Glycerol solution was substituted for human blood as a more readily available working fluid, based on our previous reports [22]–[24]. Each fluid was perfused in the CPB system, and the viscosities were measured using a vibrating viscometer (SV-10; A & D. Co., Ltd., Tokyo, Japan). The glycerin solution was prepared by adding glycerin to water, and then stored in a venous reservoir. Glycerin solution samples with viscosities of 1.88 mPas (20.7 °C), 2.84 mPas (18.8 °C), and 3.60 mPas (17.7 °C) were prepared by dilution with water. Glycerin solution viscosity corresponds to a viscosity of diluted blood, which is generally used in CPB cases [27]. Human erythrocyte solution (Cosmo Bio. Co., Ltd., Tokyo, Japan) was used with a physiological saline solution. In particular, a sample with a viscosity of

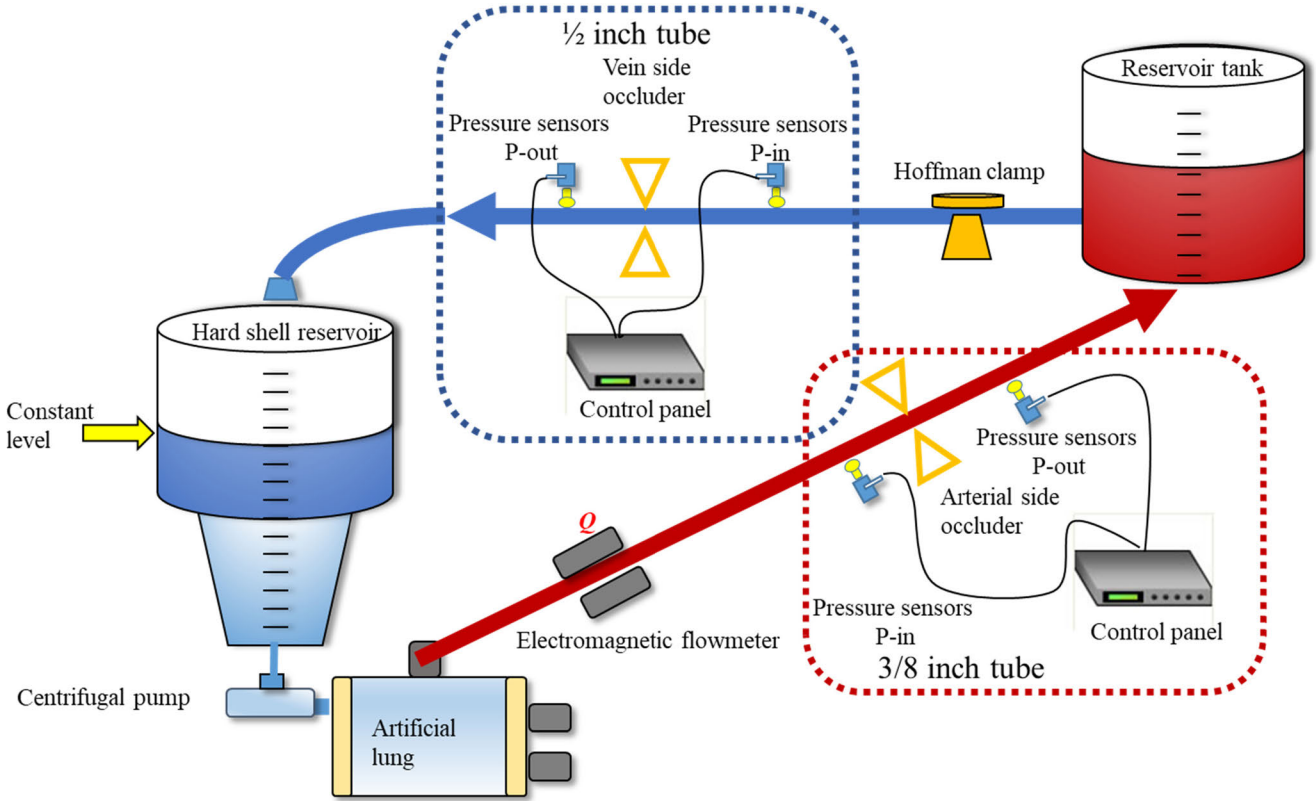

FIGURE 1. CPB system incorporating centrifugal pump. Differential pressures of the occluders on venous and arterial line sides were measured and adjusted to the maintain reservoir level.

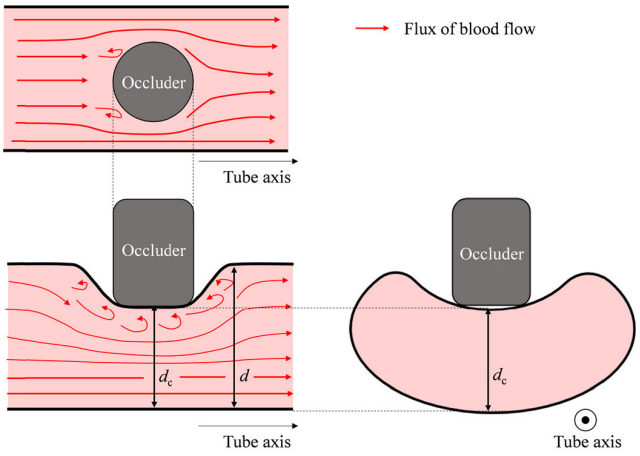

FIGURE 2. Schematic diagram of separating flow caused by occluder closure. The red lines indicate blood flux; *d* is the diameter of the pressed tube, and *dc* is the diameter of the tube.

2.66 mPas (24.3 °C) and hematocrit level of 31.0% was prepared.

C. PERFUSION EXPERIMENTS

In the in vitro experiments, the two types of fluids described in section II.B (EXPERIMENTAL FLUIDS), namely, the glycerin solutions and human erythrocyte solution, were perfused through the oxygenator using a centrifugal pump. The rotation speed of the centrifugal pump was 1700–2200 rpm. The Hoffman clamp was placed in the circuit tube on the venous line side. The occluders in the arterial and venous line sides were operated so that the venous reservoir level was always maintained at a steady level. In this study, the venous reservoir level stabilization indicates that the flow rates in the occluders on the arterial and venous line sides are equal. When the occluder is fully opened, the flow rate is 3 L/min. In the experiment, the flow rate was reduced by closing the occluder on the venous line in 5% decrements. At the same time, the occluder on the arterial line side was manipulated to equalize the flow rates of both sides and reservoir level. In the same manner, the occluder on the arterial line was then closed in 5% decrements, and the occluder on the venous line was adjusted to equalize the reservoir level. The occluder inlet and outlet pressures and average flow rate were recorded for each adjustment of the opening ratio of the occluder. These experimental procedures were carried out to evaluate dispersion in the glycerin solutions with three different viscosities and human erythrocyte solutions. The measurements were repeated five times for each glycerin and human erythrocyte solution.

D. VORTEX FORMATION VISUALIZATION

Fig. 4 shows an additional CPB system for visualizing the separation flow generated by the occluder closure.

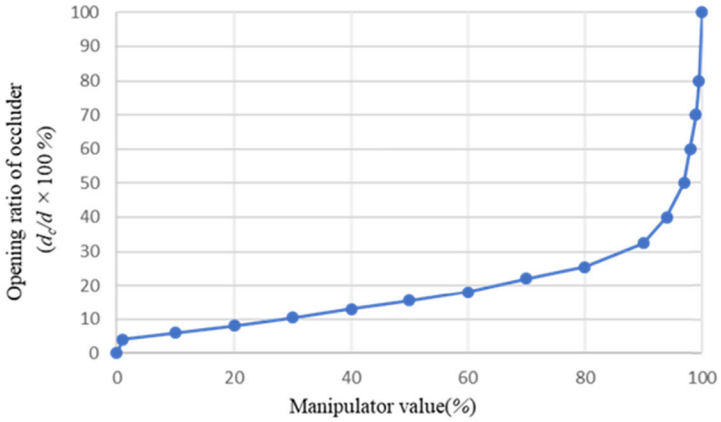

(a) manipulator value and opening ratio of occluder

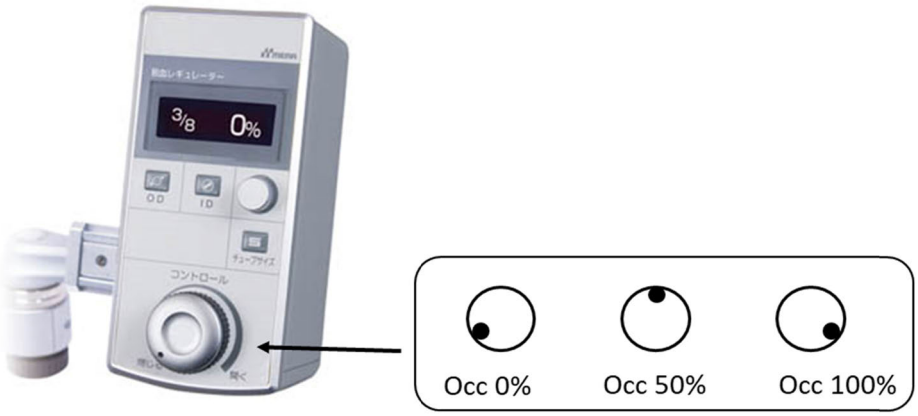

(b) manipulator value

FIGURE 3. Definition of the opening ratio of occluder. Image (a) shows the relationship between the manipulator value and opening ratio of occluder (Data published by Senko Medical Instrument Mfg. Co., Ltd., (Tokyo, Japan)). The vertical axis represents the opening ratio of occluder, and the horizontal axis represents the manipulator value. Image (b) shows the manipulator value controlled by the knob handle, which is shown on display. The occluder has an exponential relationship between the opening ratio of occluder and the manipulator value, as shown in the blue line in (a), to facilitate flow rate control by an operator.

The perfusion circuit was composed of a centrifugal pump (CX-SL45X; Terumo Cardiovascular Systems Corp, Tokyo, Japan) and electromagnetic blood flow meter (FD-M5AT, Flow range 0-10 L/min, Repetition accuracy 10s: ±1%; Keyence Corp, Tokyo, Japan), which were connected using polyvinyl chloride tubes. The glycerin solution with added polystyrene beads (Daiyaion^{TM}; Mitsubishi Chemical Holdings Corp, Tokyo, Japan) was used as perfusate. The perfusate in the system was illuminated using an infrared laser (Z-LASER; Edmund Optics® Headquarters, New Jersey, USA) and imaged using a Universal Serial Bus (USB) camera (LU105M-IO; Lumenera Corp, Canada). To visualize the polystyrene beads flowing through the blood circuit, a transparent occluder was crafted. The material of the crafted occluder is acrylic resin. The size and shape of the occluder are the same as those of occluder HAS-RH200, manufactured by Senko Inc. The crafted acrylic occluder was attached to the tube on the venous side, as shown in Fig. 4. A water level tube was installed between the acrylic occluder and HAS-RH200 to confirm that the acrylic occluder had the same opening ratio of occlusion as that of HAS-RH200. If the water level of the cylinder is stable, the flow rate to the acrylic occluder is the same as that of HAS-RH200. Therefore, the opening ratio of the occluder can be determined by HAS-RH200, and the flow can be visualized by the acrylic occluder. Moreover, the occluder was closed in steps of 5%, and the same measurement procedure as described in the previous section was repeated. The captured images were analyzed using fluid measurement software (Flow-PVI v6.01; Library Co., Ltd., Tokyo, Japan). As a measurement method, the sequential dismissal method for the accumulation of luminance differences was chosen. The tracking parameters were set to 15 × 15 pixel grid spacing, 11-pixel tracking interval, and 11-pixel reference size for image analysis.

III. MATHEMATICAL MODEL

In this section, we derive a simple model from the Navier-Stokes equation that can be applied to automatically control

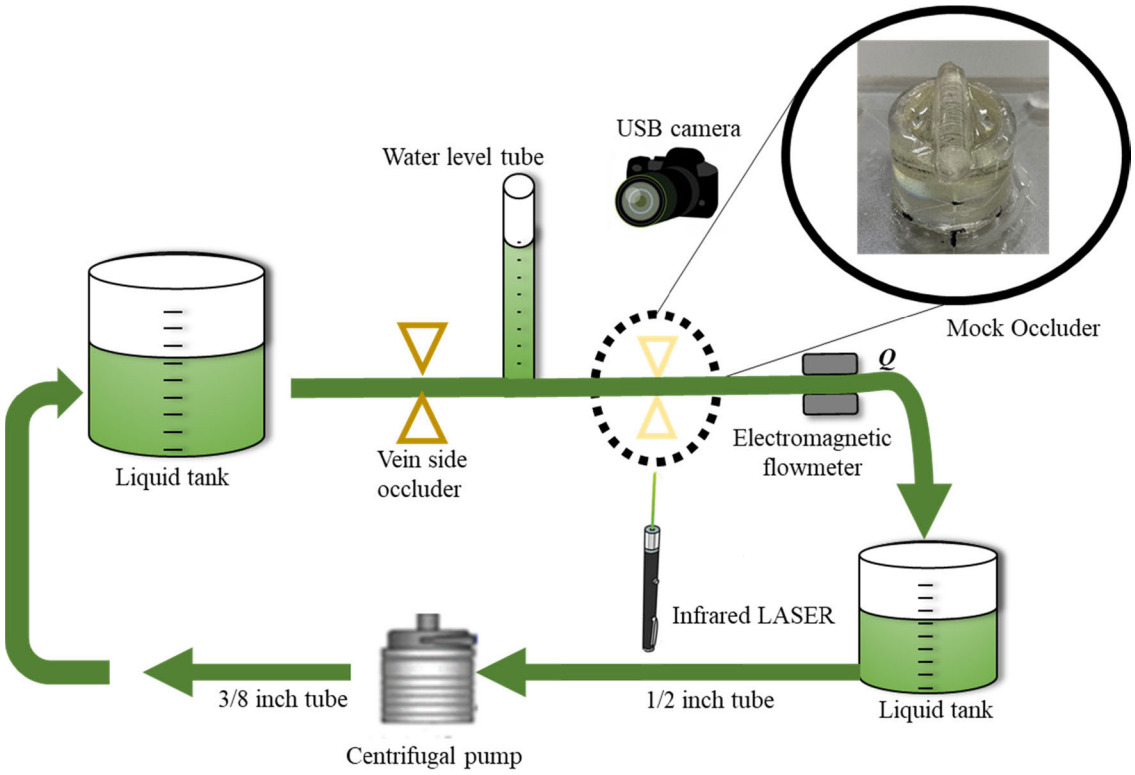

FIGURE 4. Perfusion circuit system for turbulence visualization. The crafted acrylic occluder equivalent to HAS-RH200 is marked by a black circle.

of the occluder in the future. To this end, we assume that the blood flow in the tube of the CPB circuit is laminar. The Navier-Stokes equation is given by the following:

$$\frac{\partial u}{\partial t}+u\frac{\partial u}{\partial x}+v\frac{\partial u}{\partial r}=F_x-\frac{1}{\rho}\frac{\partial p}{\partial x}+\frac{\mu}{\rho}\left(\frac{\partial^2 u}{\partial^2 x}+\frac{1}{r}\frac{\partial u}{\partial r}+\frac{\partial^2 u}{\partial r^2}\right), \tag{1}$$

$$\frac{\partial v}{\partial t}+u\frac{\partial v}{\partial x}+v\frac{\partial v}{\partial r}=F_r-\frac{1}{\rho}\frac{\partial p}{\partial r}+\frac{\mu}{\rho}\times\left(\frac{\partial^2 v}{\partial^2 x}+\frac{1}{r}\frac{\partial v}{\partial r}-\frac{v}{r^2}+\frac{\partial^2 v}{\partial r^2}\right), \tag{2}$$

where t is time; x is the axial position of the tube; r is the radial distance; u and v are the flow velocity in the x and r directions, respectively; F_x and F_r are volume forces; ρ is the density of the fluid; μ is the viscosity, and p is the pressure. For simplification, the blood flow in the circuit is assumed to be a steady flow through a tube with a constant cross-sectional area, and the volume force is ignored ($F_x = F_r = 0$). From the steady-state flow assumption, the time derivative terms become 0, $v = 0$, and $\partial u/\partial x = (\partial^2 u)/(\partial^2 x) = 0$; therefore, (1) and (2) are rewritten as the following equations:

$$r\frac{\partial p}{\partial x}=\mu\frac{d}{dr}\left(r\frac{du}{dr}\right), \tag{3}$$

$$0=-\frac{1}{\rho}\frac{\partial p}{\partial r}. \tag{4}$$

By integrating both sides of the Equation (3) twice about r, we obtain the following equation:

$$u=\frac{1}{4\mu}\left(\frac{dp}{dx}\right)r^2+\frac{C_1}{\mu}\ln r+C_2. \tag{5}$$

Because u is finite, $C_1 = 0$. C_2 can be obtained using the condition that $u = 0$ for the tube wall ($r = r_0$). Then, the velocity in this flow is given by

$$u=\frac{1}{4\mu}\left(\frac{dp}{dx}\right)\left(r_0^2-r^2\right). \tag{6}$$

The flow rate Q is obtained by multiplying the flow velocity u by the small cross-sectional area, $2\pi rdr$, and integrating with r as the following:

$$Q=\int_0^{r_0}u2\pi rdr=-\frac{\pi r_0^4}{8\mu}\frac{dp}{dx}. \tag{7}$$

Therefore, the relationship between the pressure loss P and Q between any two points is found by

$$Q=-\frac{\pi r_0^4}{8\mu}\frac{P}{l}, \tag{8}$$

where l is the length of the tube, and this equation is known as the equation of Hagen-Poiseuille flow.

We then formulated the relationship between the manipulator value (see Fig. 2) and the flow rate based on Equation (8). The variables are henceforth subscripted by i (arterial, i = a; and venous, i = v) to distinguish the arterial and venous lines

of the CBP circuit. Here, $Q_{0,i} = -P_i/(R_i + \Delta R_{0,i})$ is the flow rate when the occluder is fully opened ($O_{cc,i} = 100\%$), where $R_i = 8\mu l_i/\pi r_{0,i}^4$ is the tube friction, and P_i is the applied pressure. The tube length l_i does not include the channel length of the occluder, and $\Delta R_{0,i}$ is the channel friction of the occluder when $O_{cc,i} = 100\%$. Because the occluder channel is sufficiently short compared to the tube length l_i, we can approximate $Q_{0,i} \approx -P_i/R_i$. When the occluder is closed, flow rate Q_i can be obtained by the following equation:

$$Q_i = -\frac{P_i}{R_i + \Delta R_i} = -\frac{\frac{P_i}{R_i}}{1 + \frac{\Delta R_i}{R_i}} \approx \frac{Q_{0,i}}{1 + \frac{\Delta R_i}{R_i}}, \tag{9}$$

where ΔR_i is the increased tube friction caused by closing the occluder. By denoting the measured pressures at the inlet and outlet of the occluder as $P_{\text{in},i}$ and $P_{\text{out},i}$, the pressure loss owing to the occluder can be expressed by $\Delta P_i = P_{\text{out},i} - P_{\text{in},i}$. Using the relationship $\Delta P_i = Q_i \Delta R_i$, (9) can be summarized in the following form

$$Q_i = -\frac{1}{R_i} Q_i \Delta R_i + Q_{0,i} = -\frac{1}{R_i} \Delta P_i + Q_{0,i}. \tag{10}$$

This equation allows us to determine unknown R_i and $Q_{0,i}$ from Q_i, $P_{\text{in},i}$ and $P_{\text{out},i}$ measured by the CPB system.

We then introduced a model that can estimate the pressure loss from the manipulator value of the occluder. Fig. 2 shows a schematic diagram of a tube pressed by an occluder. When the blood flows through the pressed tube, separating flow occurs, causing a pressure loss, as shown in the figure. It is difficult to theoretically derive the pressure loss ΔP_i caused by closing the occluder because the cross-section of the tube compressed by the occluder is complexly deformed, as shown on the right side of Fig. 2. In this study, for simplicity, we assumed that ΔP_i is inversely proportional to the opening ratio of occluder d_c/d (see Fig. 2 and Fig. 3). Figure 3 shows the relationship between the manipulator value and the opening ratio of occluder. Let us define a function that links the manipulator value of occluder, $O_{cc,i}$, with opening ratio of occluder, d_c/d, as the following:

$$\frac{d_c}{d} = f(O_{cc,i}), \tag{11}$$

ΔP_i can then be expressed by the following equation:

$$\Delta P_i = \Delta R_i Q_i = \frac{1}{f(O_{cc,i})} Q_i, \tag{12}$$

where ΔR_i is the loss factor. ΔR_i can then be defined by the following equation:

$$\frac{1}{\Delta R_i} = \frac{Q_i}{\Delta P_i} = f(O_{cc,i}), \tag{13}$$

Finally, substituting (13) into (10) and solving for Q_i gives the following equation representing the relationship between manipulator value $O_{cc,i}$ and flow rate Q_i.

$$Q_i = \frac{Q_{0,i}}{\left(1 + \frac{1}{R_i} \frac{1}{f(O_{cc,i})}\right)} = \frac{Q_{0,i} R_i f\left(O_{cc,i}\right)}{R_i f\left(O_{cc,i}\right) + 1} \tag{14}$$

In this study, we employed occluder manufactured by Senko Inc. Fig. 3 shows the relationship between the manipulator value and the opening ratio of the occluder employed. According to this figure, the manipulator value and opening ratio of the occluder d_c/d can be expressed by an exponential function using the occluder opening $O_{cc,i}$ as follows.

$$\frac{d_c}{d} = f\left(O_{cc,i}\right) = A_i \left\{\exp\left(K_i O_{cc,i}\right) - 1\right\}, \tag{15}$$

where A_i and K_i are calibration coefficients. ΔR_i and Q_i thus can be estimated by substituting right-hand side of (15) for $f\left(O_{cc,i}\right)$ in Equations (13) and (14). Here, the calibration coefficients in (13) and (15) can be determined by fitting Equation (13) to the measured data ($\Delta P_i/Q_i$) at different $O_{cc,i}$.

The model can be applied to other occluders by replacing $f\left(O_{cc,i}\right)$ with an occluder-dependent function that can express the relationship between the manipulator value, $O_{cc,i}$, and the opening ratio of occluder, d_c/d. A two-step estimation allows us to separate the fluid mechanical parameters and occluder-dependent calibration parameters, as shown in (10) and (13). This separation provides an advantage to generalize the model to other occluders.

A. PARAMETER DETERMINATION AND VERIFICATION

The calibration coefficients Q_0 and R_i were determined by the least square method. The parameters A_i and K_i were determined using a non-linear regression method (Levenberg–Marquardt algorithm). The fitting accuracy of the proposed model (10)–(13) and (14) was evaluated using the coefficient of determination.

Leave-one-out cross-validation was then carried out to examine the validity of the determined parameters and the prediction accuracy of the proposed model. The flow rate prediction accuracy and its systematic errors were evaluated using the coefficient of determination and Bland-Altman analysis, respectively.

Here, regression and Bland–Altman plot analyses were conducted using statistical software R and the graphical user interface Easy R (Saitama Medical Center, Jichi Medical University, Saitama, Japan). A significance level of 0.01 was assumed in all the statistical tests ($p < 0.01$).

IV. RESULTS

The individual analyses conducted on the three glycerin solutions at different viscosities (1.88, 2.84, and 3.60 mPas) indicate that the linear flow-pressure model was well fitted with the measured data ($R^2 > 0.977$ (venous line) and $R^2 > 0.983$ (arterial line); $p < 0.01$), as shown in Fig. 5 a and b.

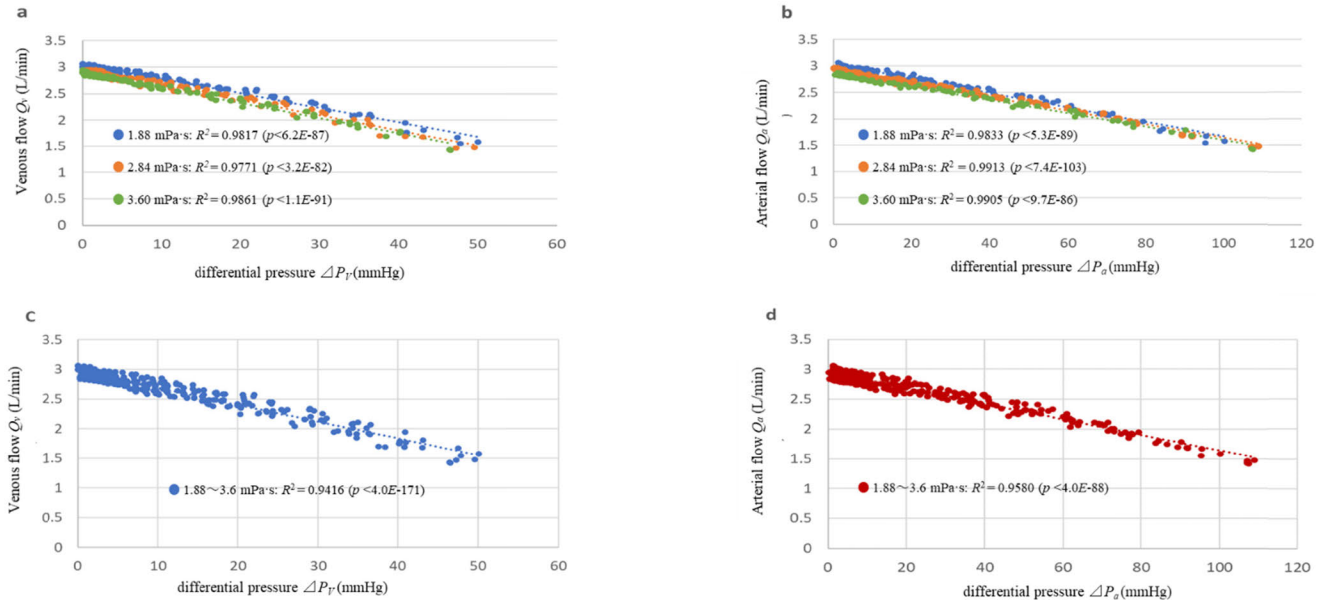

FIGURE 5. Relationship between differential pressure and flow rate for glycerin solutions. Circular markers indicate measured data, whereas filled color distinguishes the viscosity level. Solid and dotted lines indicate the fit obtained using the proposed model described in (10). Here, (a) and (b) depict measured data and model fit to (10) observed on venous- and arterial-line sides, respectively. Images (c) and (d) depict fitting to equation (10) for all measured data with respect to viscosity on venous- and arterial-line sides, respectively.

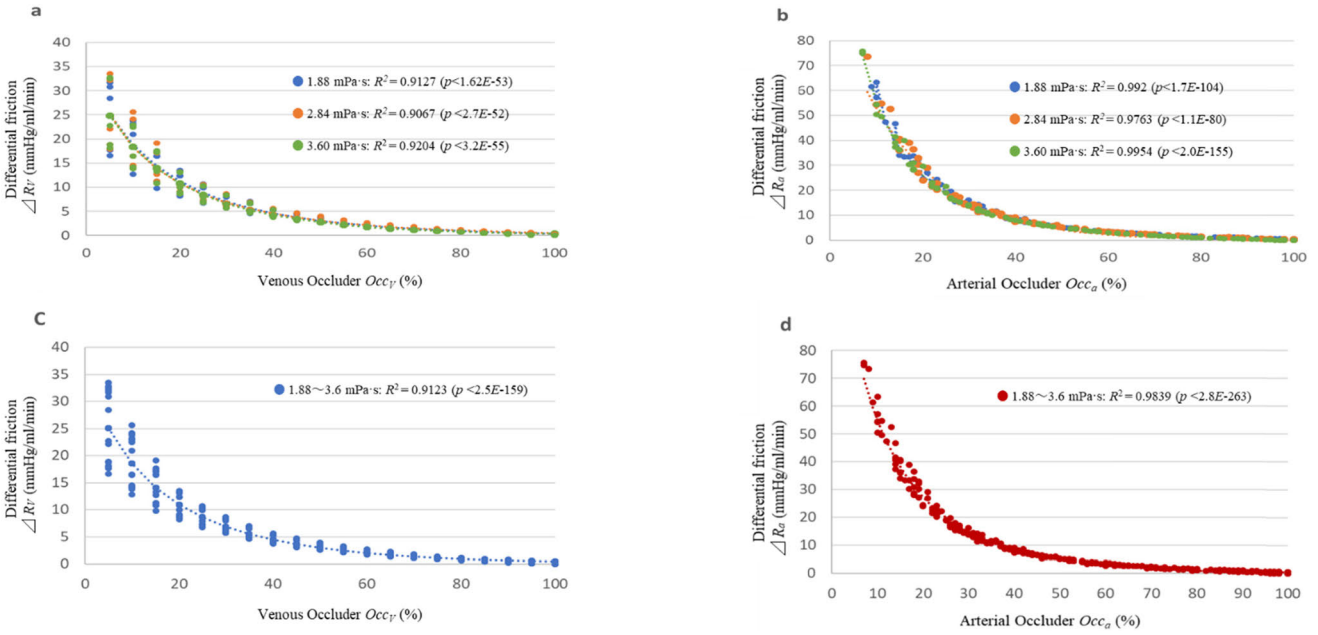

FIGURE 6. Relationship between differential pressure and flow rate for glycerin solutions. Circular markers indicate measured data, whereas filled color indicates viscosity. Solid and dotted lines indicate the fit obtained using the proposed model described in (13). Images (a) and (b) depict measured data and fits of the model (13) observed on venous- and arterial-line sides, respectively. In these figures, the models were respectively fitted to the data measured from glycerin solutions with different viscosities. Images (c) and (d) depict the fit of the model to (13) for all measured data on venous- and arterial-line sides, respectively.

A combined analysis also showed that the model was well fitted to the measured data ($R^2 > 0.942$ (venous line) and $R^2 > 0.958$ (arterial line); $p < 0.01$), as shown in Fig. 5 c and d. Fig. 6 shows measured ΔR_a and ΔR_v modified by the manipulator values of the occluders ($O_{cc,v}$ and $O_{cc,a}$) and the regression lines of the exponential occlusion-pressure model (13). The individual analyses of the three glycerin solutions viscosities show that the exponential occlusion-pressure model was well fitted to the measured data ($R^2 > 0.994$ (venous line) and $R^2 > 0.995$ (arterial line); $p < 0.01$), as shown in Fig. 6a and b. The combined analysis is also well fitted to the measured data ($R^2 > 0.997$ (venous line)

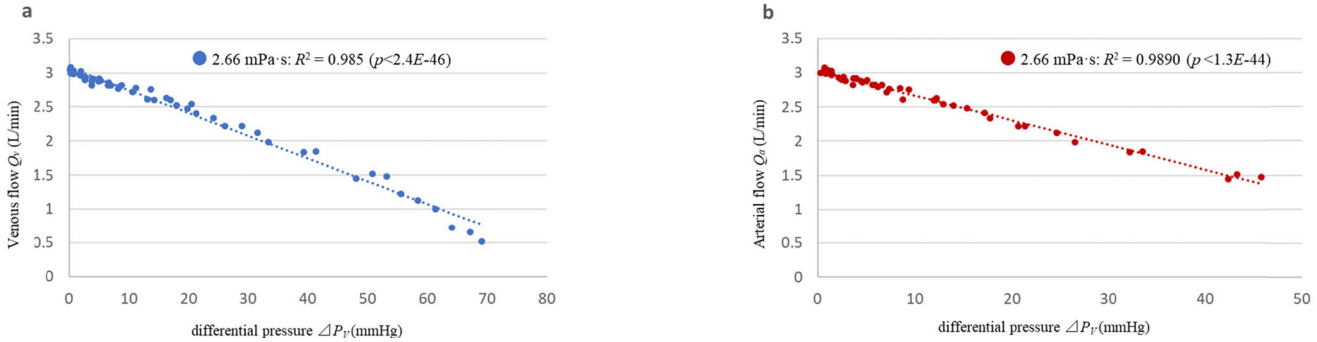

FIGURE 7. Relationship between the occluder differential pressure and flow rate for blood. Circular markers indicate measured data, whereas dotted lines indicate fits to (10) on (a) venous-line and (b) arterial-line sides.

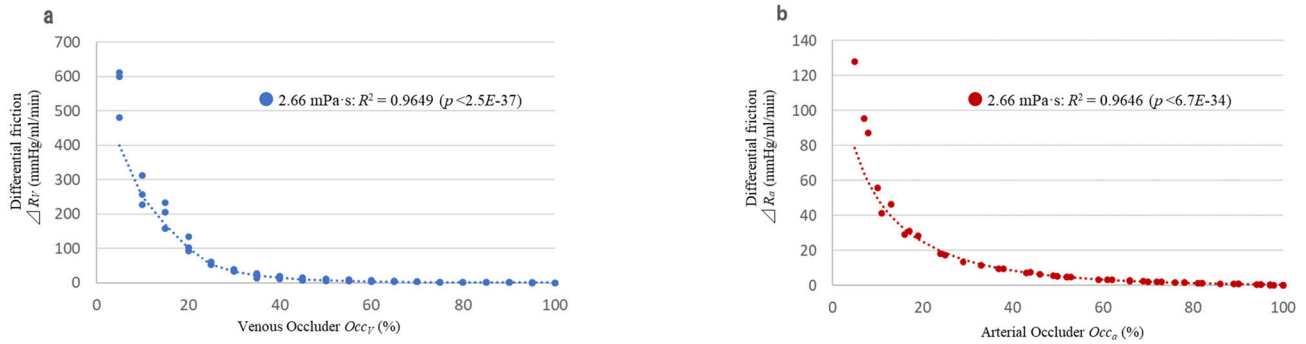

FIGURE 8. Relationship between differential pressure and opening ratio of occluder for blood. Circular markers indicate measured data, whereas dotted lines indicate fits to (13) on (a) venous-line and (b) arterial-line sides.

TABLE 1. Calibration Parameters of the Proposed Model.

	A_i		K_i		R_i		$Q_{0,i}$	
	Venous side i=v	Arterial side i=a	Venous side i=v	Arterial side i=a	Venous side i=v	Arterial side i=a	Venous side i=v	Arterial side i=a
1.88 mpa·s	0.0669	0.0451	0.0344	0.0331	0.0276	0.0137	3.0611	3.0422
2.84 mpa·s	0.1039	0.0321	0.027	0.0386	0.029	0.0129	2.9625	2.9339
3.6 mpa·s	0.0777	0.0137	0.034	0.0644	0.0287	0.0125	2.9002	2.8597
Total 3 level viscosity	0.0784	0.0346	0.0324	0.038	0.0282	0.013	2.9715	2.9461
Blood (2.66 mpa·s)	0.0196	0.0323	0.0451	0.0392	0.0334	0.036	3.0803	3.0275

and $R^2 > 0.999$ (arterial line); $p < 0.01$), as shown in Fig. 6 c and d. The experimental results and regression lines are shown in Figs. 7 and 8, respectively. Fig. 7 shows that the linear flow-pressure model regression was well fitted to the measured data on the venous- and arterial-line sides ($R^2 = 0.985$ and $R^2 = 0.997$, respectively; both produced $p < 0.01$). Moreover, the exponential occlusion-pressure model was well fitted to the measured data on the venous- and arterial-line sides ($R^2 = 0.989$ and $R^2 = 0.988$, respectively; both with $p < 0.01$), as shown in Fig. 8.

Table 1 lists the proposed model calibration parameters determined by fitting the estimated data to the measurements (see Materials and Methods; Mathematical Model). Based on these parameters, the flow rate from the opening ratio of the occluder can be estimated using (14). Fig. 9 shows the relationship between the opening ratio of the occluder ($O_{cc,v}$, $O_{cc,a}$) and flow rates (Q_v, Q_a), in addition to the fitted lines based on (14). These results show significant high coefficients of determination between the estimated and measured values for the venous- and arterial-line sides ($R^2 = 0.956$ and $R^2 = 0.993$, respectively; both with $p < 0.01$).

Additionally, leave-one-out cross-validation was carried out to verify the proposed method prediction accuracy. Fig. 10 shows the predicted Q_i plotted against the measured

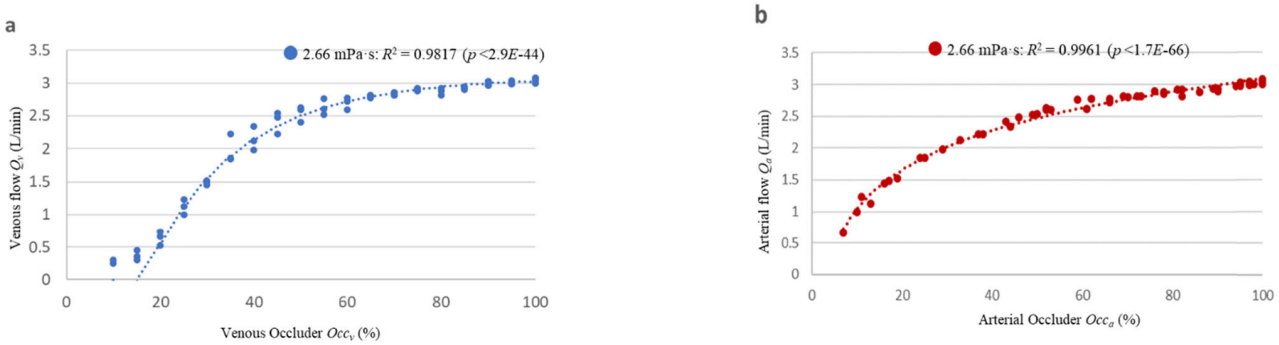

FIGURE 9. Relationship between opening ratio of the occluder and flow rate for blood. Circular markers indicate measured data, whereas dotted lines indicate fits to (14) on (a) venous-line and (b) arterial-line sides.

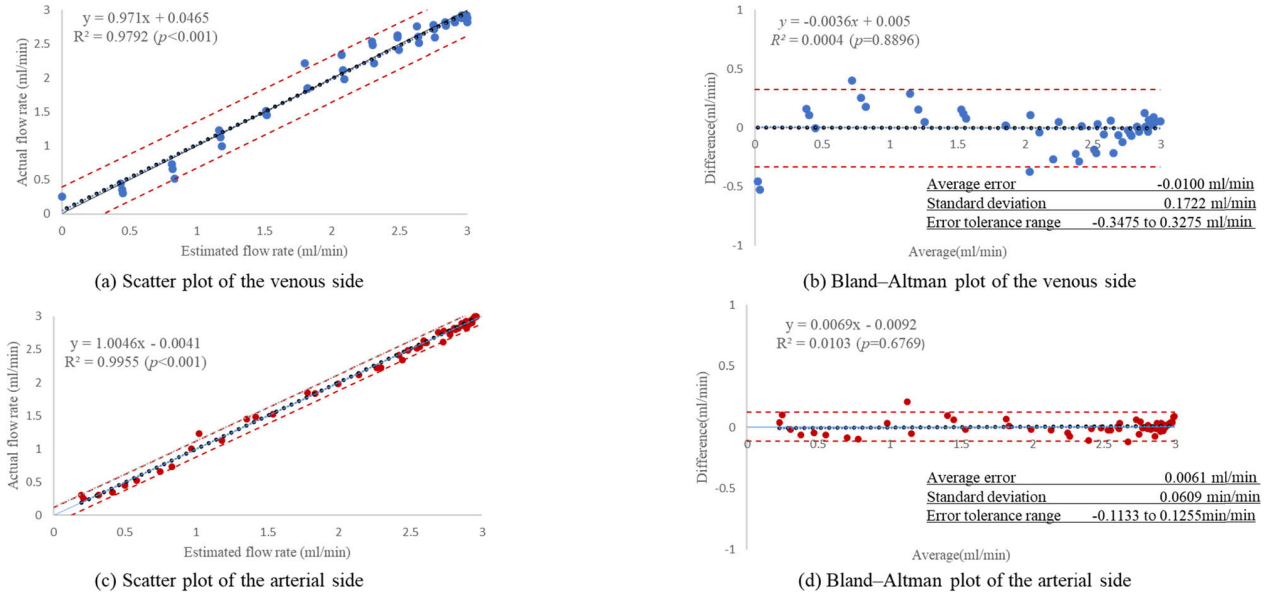

FIGURE 10. Prediction accuracy of the proposed model (14) evaluated by leave-one-out cross-validation. Images (a) and (c) depict scatter plots between the predicted and measured flow rates. Solid blue lines are lines of equality; black dotted lines indicate linear fitting to the plot points; red dotted lines denote 95% confidence interval of predicted values. Images (b) and (d) depict Bland–Altman plots. Blue solid lines denote bias (mean of difference); black dotted lines indicate linear fitting to plot points; red dotted lines denote 95% confidence interval of bias.

flow rate. The coefficient of determination obtained from the venous-line side using cross-validation is 0.979 ($p < 0.01$) (Fig. 10a), and that of the arterial-line side is 0.996 ($p < 0.01$) (Fig. 10c). Bland–Altman analysis was then used to evaluate the prediction accuracy of (14), as shown in Figs. 10b and 10d. There are no constant errors on the arterial- and venous-line sides given that zero was included in the 95% confidence interval. Further, proportional error was not found given that the R^2 p-values on the venous and arterial sides are 0.890 and 0.677, respectively. These results indicate that systematic errors are minimal.

The relationship between the flow rate and manipulator values of the occluder was dichotomized in the venous side (see Fig. 9). We thus visualized the flow in the venous side to investigate the cause of this dichotomy. Fig. 11 shows that occluder closure resulted in the perfusate separation. The separated flows were situated at the occluder restrictor upper rear part, and further closure promoted the spread of the vortex throughout the blood circuit behind the occluder. The onset of exfoliation flow occurred at 95% closure in the first, second, and fifth trials and 90% in the third and fourth trials. The spread of the vortex throughout the blood circuit occurred at 80% closure in the second trial; 75% closure in the first, fourth, and fifth trials; and 70% closure in the third trial.

V. DISCUSSION

This study evaluated the influence of the manipulator value of the occluder on the differential pressure. We assumed that the relationship between the manipulator value, $O_{\mathrm{cc},i}$, and opening ratio of the occluder d_c/d is exponential, and d_c/d is inversely proportional to tube friction ΔR_i. This assumption is justified by the high accuracy of the fitting to the measured data of both glycerin solutions and blood (see Fig. 6). To facilitate flow control by an operator, CPB occluders are commonly configured in such a way that the relationship

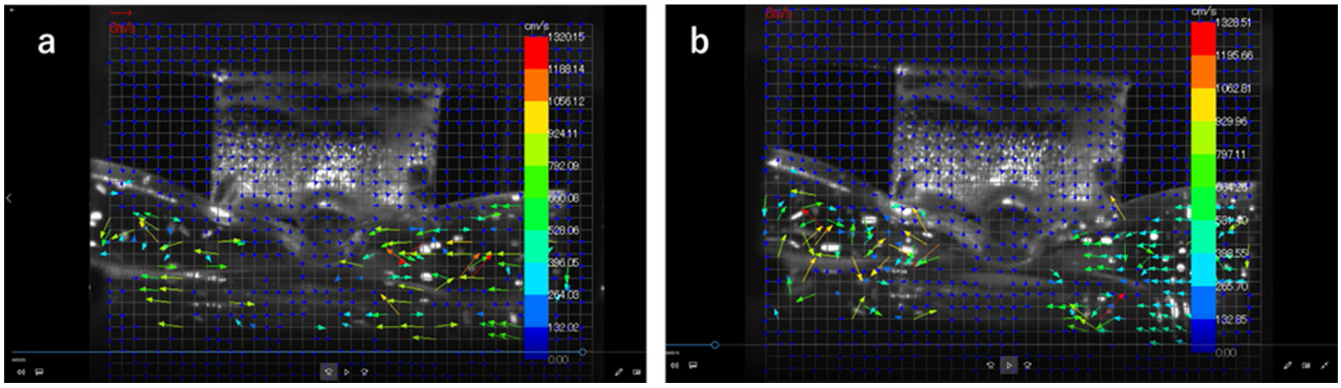

FIGURE 11. Arrows indicate flow direction, and their colors denote flow rate. Image (a) shows flow when opening ratio of occluder is in 90–95% range with separation flow generated at the top of the circuit. Image (b) shows flow when opening rate of occluder is in a range of 70–80% with separation flow generated through the entire circuit.

between the manipulator value, $O_{\mathrm{cc},i}$, and the opening ratio of the occluder, d_c/d, forms a monotonic non-linear function $d_c/d = f(O_{cc,i})$. The proposed model can be generalized to other occluders by replacing $f(O_{cc,i})$, expressed by Equation (11) in this study, to an appropriate monotonic non-linear function.

The fitting results confirm that the relationship between the differential pressure and flow rate, in addition to that between the differential pressure and opening ratio of the occluder, is not significantly influenced by changes in the fluid viscosity (see Figs. 5 and 6 a.b.c.d). These results indicate that it is unnecessary to include viscosity as a parameter of the model.

The analysis result showed that the correlation on the venous side was lower than that on the arterial side. This is because the measured flow rates dichotomized (see Fig. 9a). To investigate the cause of this, we visualized the flow around the occluder. By visualizing the venous side, we found that the spread of the vortices in the entire blood circuit does not occur at a specific opening ratio of the occluder. This observation suggests that Hopf bifurcation is occurring in the blood circuit [28], which is not controllable and can cause a certain prediction error of the flow rate. This error is unavoidable because our model focuses on steady-state flow. Therefore, an assisted cardiopulmonary manipulation control system to be developed in the future requires combining feedforward control using the proposed model to shift between the steady states and feedback control to absorb error caused by the turbulent flow.

In this study, we assumed the working fluid to be a simple viscous fluid (Newtonian fluid); however, the viscosity of actual blood nonlinearly changes and affects the pressure drop. Nonetheless, the blood and glycerin approximated by the same model equation demonstrated high coefficients of determination, where $R^2 > 0.998$ ($p < 0.01$) for the venous line and $R^2 > 0.988$ ($p < 0.01$) for the arterial line. These results indicate that the proposed model can be applied to blood.

The parameters were determined using the experimental data obtained from the perfusion system connected by tubes with a diameter of 0.5 and 0.375 on the venous- and arterial-line sides, respectively. The system configuration and difference between the non-Newtonian fluid characteristics may have an influence on the calibration parameters. For example, the differences between the occluder positions and circuit lengths may alter the flow velocity distribution, which has an influence on the differential pressure [29]. Therefore, the three parameters in the proposed model require tuning to the specific CPB system configuration.

By building an inverse model of the proposed model, $O_{\mathrm{cc},i}$ can be determined from the desired flow rate. This inverse model can be easily derived owing to the simplicity of the proposed model. Therefore, the proposed model can be used for feedforward control to shift the steady-state, which serve as a basis for the development of control methods and the realization of assisted cardiopulmonary manipulation control systems. In the future, transient responses of physiological functions need to be considered. By combining feedback control and feedforward control to absorb the errors caused by such transient responses, a cardiopulmonary manipulation support control system can be realized. Furthermore, to realize a control system for various scenarios in cardiac surgery, the technology to monitor the reservoir level in real-time is required, which is the next stage of research. By building an inverse model of the proposed model, Occ can be determined from the desired flow rate, and the steady state can be shifted. This model is simple and it is easy to construct the inverse model. Therefore, the proposed model can serve as a basis for the development of control methods and the realization of assisted cardiopulmonary manipulation control systems.

VI. CONCLUSION

This study developed a model to enable estimation of flow rate from the manipulator value of the occluder used in the CPB circuit. The results demonstrate that the proposed model can accurately estimate the relationship between the differential pressure, flow rate, and opening ratio of the occluder for non-Newtonian fluids perfused in the circuit. The results of this study can serve as basis for further development of

cardiopulmonary operation interlocking systems as well as simplification of occluder operation.

REFERENCES

[1] *Standards of practice (revised)*, American Academy of Cardiovascular Perfusion, Austin, TX, USA, 1994
[2] K. Balasaraswathi, S. N. Glisson, A. A. El-Etr, and C. Azad, "Effect of priming volume on serum catecholamines during cardiopulmonary bypass," *Can. Anaesthetists Soc. J.*, vol. 27, no. 2, pp. 135–139, Mar. 1980, doi: 10.1007/BF03007775.
[3] N. L. Mills and J. L. Ochsner, "Massive air embolism during cardiopulmonary bypass. Causes, prevention, and management," *J. Thorac. Cardiovasc. Surg.*, vol. 80, no. 5, pp. 708–717, 1980, doi: 10.1016/S0022-5223(19)37716-5.
[4] J. H. Gibbon, "The maintenance of life during experimental occlusion of the pulmonary artery followed by survival," *Surg. Gynecol. Obstet.*, vol. 9, pp. 602–614, 1Dec. 939.
[5] O. F. Jenkins, R. Morris, and J. M. Simpson, "Australasian perfusion incident survey," *Perfusion*, vol. 12, no. 5, pp. 279–288, Sep. 1997, doi: 10.1177/026765919701200502.
[6] B. L. Mejak, A. Stammers, E. Rauch, S. Vang, and T. Viessman, "A retrospective study on perfusion incidents and safety devices," *Perfusion*, vol. 15, no. 1, pp. 51–61, Jan. 2000, doi: 10.1177/026765910001500108.
[7] J. Reason, "Human error: Models and management," *Western J. Med.*, vol. 172, no. 6, pp. 393–396, Jun. 2000, doi: 10.1136/ewjm.172.6.393.
[8] M. Kurusz and D. R. Wheeldon, "Risk containment during cardiopulmonary bypass," *Semin. Thorac. Cardiovasc. Surg.*, vol. 2, no. 4, pp. 400–409, 1990t.
[9] N. Momose, R. Yamakoshi, R. Kokubo, T. Yasuda, N. Iwamoto, C. Umeda, I. Nakajima, M. Yanagisawa, and Y. Tomizawa, "Development of a new control device for stabilizing blood level in reservoir during extracorporeal circulation," *Perfusion*, vol. 25, no. 2, pp. 77–82, Mar. 2010, doi: 10.1177/0267659110368306.
[10] Y. Niimi, S. Murata, Y. Mitou, and Y. Ohno, "Use of a novel drainage flow servo-controlled CPB for mitral valve replacement in a Jehovah's witness," *Perfusion*, vol. 33, no. 6, pp. 490–492, Sep. 2018, doi: 10.1177/0267659118763036.
[11] J. P. Montoya, S. I. Merz, and R. H. Bartlett, "Significant safety advantages gained with an improved pressure-regulated blood pump," *J. Extra Corpor. Technol.*, vol. 28, no. 2, pp. 71–78, 1996.
[12] R. M. Bass and D. B. Longmore, "Cerebral damage during open heart surgery," *Nature*, vol. 222, no. 5188, pp. 30–33, Apr. 1969, doi: 10.1038/222030a0.
[13] R. E. Hannemann and R. G. Barile, "Bubble formation in the roller infusion pump," *Am. J. Dis. Child.*, vol. 125, no. 5, pp. 706–708, 1973, doi: 10.1001/archpedi.1973.04160050060011.
[14] J. P. Mandl, "Comparison of emboli production between a constrained force vortex pump and a roller pump," *AmSECT Proc.*, vol. 5, pp. 27–31, Aug. 1977.
[15] M. M. Faghih and M. K. Sharp, "Evaluation of energy dissipation rate as a predictor of mechanical blood damage," *Artif. Organs*, vol. 43, no. 7, pp. 666–676, Jul. 2019, doi: 10.1111/aor.13418.
[16] A. Fukaya, Y. Shiraishi, Y. Inoue, A. Yamada, G. Sahara, T. Kudo, Y. Aizawa, and T. Yambe, "Development and accuracy evaluation of a degree of occlusion visualization system for roller pumps used in cardiopulmonary bypass," *J. Artif. Organs*, Sep. 2020, doi: 10.1007/s10047-020-01211-x.
[17] J. Kolff, J. B. McClurken, and J. B. Alpern, "Beware centrifugal pumps: Not a one-way street, but a potentially dangerous siphon," *Ann. Thorac. Surg.*, vol. 50, no. 3, p. 512, 1990, doi: 10.1016/0003-4975(90)90522-8.
[18] J. Kolff, R. N. Ankney, D. Wurzel, and R. Devineni, "Centrifugal pump failures," *J. Extra Corpor. Technol.*, vol. 28, no. 3, pp. 118–122, 1996.
[19] K. F. Poulter, "The calibration of vacuum gauges," *J. Phys. E, Sci. Instrum.*, vol. 10, no. 2, pp. 112–125, 1977, doi: 10.1088/0022-3735/10/2/002.
[20] K. F. Poulter, "Vacuum gauge calibration by the orifice flow method in the pressure range 10-4-10 pa," *Vacuum*, vol. 28, no. 3, pp. 135–141, 1978, doi: 10.1016/S0042-207X(78)80240-1.
[21] H. M. Akram, M. Maqsood, and H. Rashid, "Development and performance analysis of a standard orifice flow calibration system," *Rev. Sci. Instrum.*, vol. 80, no. 7, Jul. 2009, Art. no. 075103, doi: 10.1063/1.3176469.
[22] S. Okahara, Z. Soh, S. Miyamoto, H. Takahashi, S. Takahashi, T. Sueda, and T. Tsuji, "Continuous blood viscosity monitoring system for cardiopulmonary bypass applications," *IEEE Trans. Biomed. Eng.*, vol. 64, no. 7, pp. 1503–1512, Jul. 2017, doi: 10.1109/TBME.2016.2610968.
[23] S. Okahara, Z. Soh, S. Miyamoto, H. Takahashi, H. Itoh, S. Takahashi, T. Sueda, and T. Tsuji, "A novel blood viscosity estimation method based on pressure-flow characteristics of an oxygenator during cardiopulmonary bypass," *Artif. Organs*, vol. 41, no. 3, pp. 262–266, Mar. 2017, doi: 10.1111/aor.12747.
[24] S. Okahara, S. Miyamoto, Z. Soh, and T. Tsuji, "Detection of echinocyte during perfusion with oxygenator based on continuous blood viscosity monitoring," *Conf. Proc. IEEE Eng. Med. Biol. Soc.*, vol. 2018, pp. 4448–4451, Dec. 2018, doi: 10.1109/EMBC.2018.8513370.
[25] L. I. Zaroff, I. Kreel, D. J. Kave, and I. D. Baronofsky, "Mechanical failure during extracorporeal circulation A method for prevention," *Surgery*, vol. 45, no. 4, pp. 645–647, 1959.
[26] F. C. Hoppensteadt and C. S. Peskin, *Modeling and Simulation in Medicine and the Life Sciences*. New York, NY, USA: Springer, Jan. 2002, pp. 7–21, doi: 10.1007/978-0-387-21571-6.
[27] R. E. Wells and E. W. Merrill, "Influence of flow properties of blood upon viscosity-hematocrit relationships," *J. Clin. Invest.*, vol. 41, no. 8, pp. 1591–1598, Aug. 1962, doi: 10.1172/JCI104617.
[28] N. D. Kazarinoff, J. E. Marsden, and M. Mc Cracken, "The Hopf bifurcation and its applications," *Bull. Amer. Math. Soc.*, vol. 83, no. 5, pp. 998–1004, 1977.
[29] M. Al-Ghoul and B. Chan Eu, "Generalized hydrodynamics and microflows," *Phys. Rev. E, Stat. Phys. Plasmas Fluids Relat. Interdiscip. Top.*, vol. 70, no. 1, Jul. 2004, Art. no. 016301, doi: 10.1103/PhysRevE.70.016301.

HIDENOBU TAKAHASHI was born in Kobe, Japan, in 1973. He received the B.Sc. degree in clinical medicine from Hiroshima University, in 2006.

From 1999 to 2018, he was a Perfusionist with Hiroshima University Hospital. He is currently a Lecturer with the Department of Medical Science and Technology, Faculty of Health Science, Hiroshima International University, Japan. His research interests include the evaluation of cardiopulmonary bypass systems, experiments, and automatic occluder control.

Mr. Takahashi is a member of the Japanese Society for Artificial Organs, the Japanese Society of Extra-Corporeal Circulation Technology, and the Japan Association for Clinical Engineers.

ZU SOH (Member, IEEE) received the B.E., M.E., and D.Eng. degrees in electrical and electronic engineering from Hiroshima University, Hiroshima, Japan, in 2006, 2008, and 2010, respectively.

From 2008 to 2013, he was a Research Fellow with the Japan Society for the Promotion of Science. He has been an Assistant Professor with the Graduate School of Advanced Science and Engineering, Hiroshima University, Japan, since 2013. His current research interests include biological signal analysis, artificial life, and biological modeling.

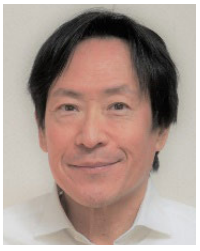

TOSHIO TSUJI (Member, IEEE) received the B.E. degree in industrial engineering and the M.E. and Dr. Eng. degrees in systems engineering from Hiroshima University, Higashihiroshima, Japan, in 1982, 1985, and 1989, respectively.

Since 2002, he has been a Professor with the Graduate School of Advanced Science and Engineering, Hiroshima University, Japan. His research interests include from engineering to human science, with focus on cybernetics, medical electronics, computational neural sciences, and, particularly, and biological Kansei modeling.

Dr. Tsuji has received 42 academic awards, including the IEEE 2003 King-Sun Fu Memorial Best Transactions Paper Award.